Supplemental Data

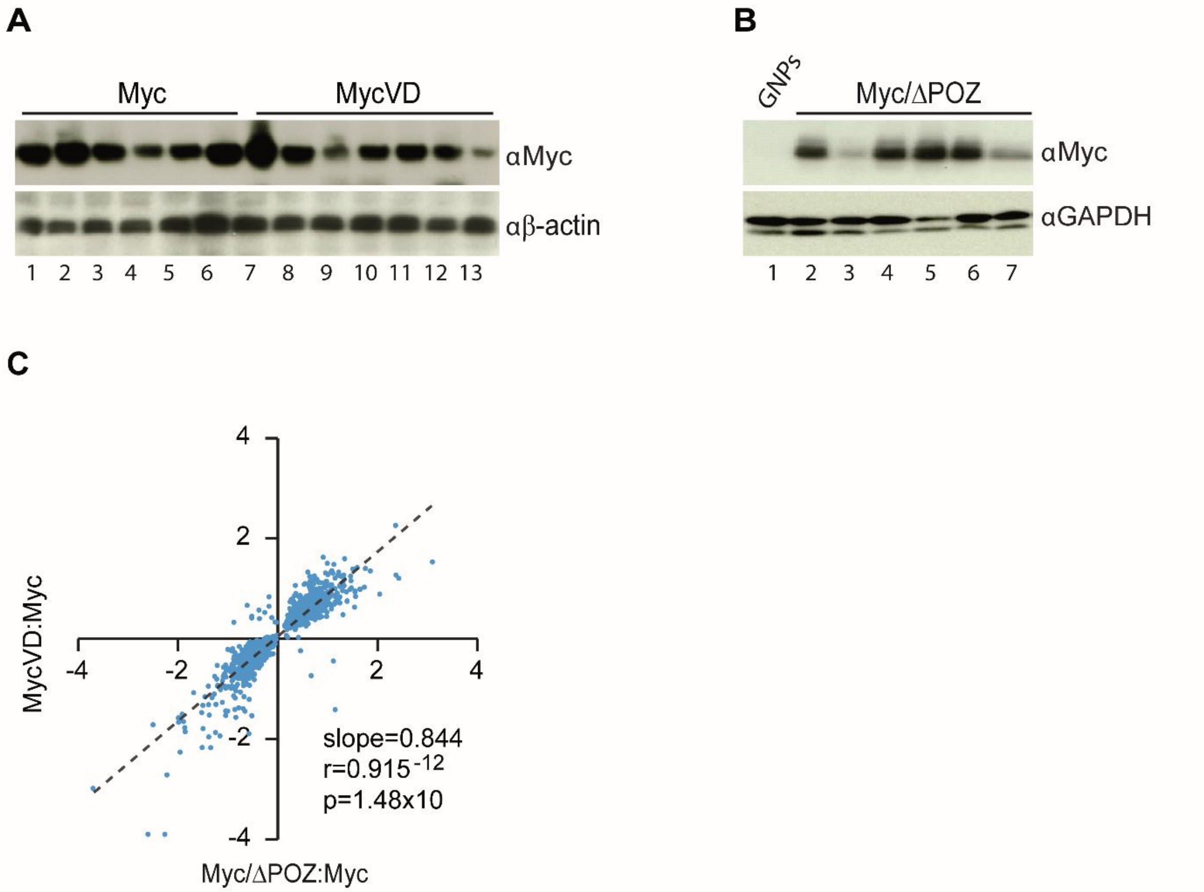

D

Geneset	NES	p value	q value
MEISSNER_NPC_HCP_WITH_ H3K4ME3_AND_H3K27ME3	1.88	0.000	0.055
MEISSNER_NPC_HCP_WITH_ H3K4ME2_AND_H3K27ME3	1.88	0.000	0.052
MIKKELSEN_MCV6_HCP_WITH_ H3K27ME3	1.88	0.000	0.054

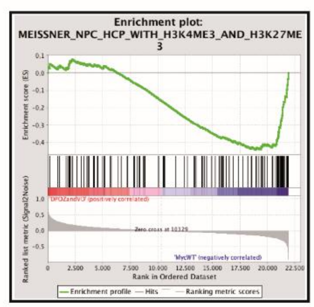

Figure S1. Characterization of Myc, MycVD and Myc/ΔPOZ tumors. Related to Figure 1. Immunoblotting of Myc expression in purified tumor cells from individually derived tumors: (A) Myc (lanes 1-6) and MycVD (lanes 7-13) tumors; (B) Myc/ΔPOZ-tumors (lanes 2-7). GNPs lacking Myc expression (lane 1). β-actin and GAPDH were used as internal controls. (C) Microarray analysis documenting the similarity in gene expression induced by MycVD versus Myc and Myc/ΔPOZ versus Myc. The diagram shows all genes which are significantly regulated in both comparisons. Every dot represents one gene (1,535 genes). Slope: regression coefficient, r: Pearson correlation coefficient, p: p value (two-tailed t-test). (D) Gene Set Enrichment Analysis (GSEA) of gene expression in Myc/ΔPOZ- and MycVD- in comparison to Myc tumors. To identify which sets of genes are commonly deregulated in Myc/ΔPOZ- and MycVD-tumors, expression data of 4 Myc/ΔPOZ- and MycVD-tumors were combined and compared to 3 control Myc/G3 MB by GSEA. List and examples of selected gene sets of down-regulated genes are shown.

Table S1. Genes upregulated in MycVD- and Myc/ΔPOZ- compared to Myc-tumors. Related to Figure 1.

Symbol	Gene name	Functional Annotation	Myc-N/A	MycVD-Myc	Myc/ΔPOZ-Myc
Alms1	Alstrom syndrome 1	Neuronal differentiation	-0.71943333	0.35940619	0.631393333
Apaf1	Apoptotic protease activating factor 1	Putative tumor suppressor	-0.36848167	0.03106167	0.156382917
Armcx1	armadillo repeat containing, X-linked 1, Alex1	Putative tumor suppressor	-0.73656667	0.02959	0.011635
Atoh1	atonal homolog 1 (Drosophila)	Neuronal differentiation	-5.37026	1.93455095	0.469189167
Cadm2	cell adhesion molecule 2	Putative tumor suppressor	-1.15808905	0.53395122	0.37777
Camk2n1	calcium/calmodulin-dependent protein kinase II inhibitor 1	Putative tumor suppressor	-2.27819667	0.46088167	0.895752917
Cd47	CD47 antigen (Rh-related antigen, integrin-associated signal transducer)	Neuronal differentiation	-1.0061775	0.32902119	0.230502708
Ctsb	cathepsin B	TGF-beta signaling	-0.30257533	0.58987295	0.387893667
Egr1	Early growth response protein 1	Neuronal differentiation	-2.81134333	1.28078905	1.110643333
Eps15	epidermal growth factor receptor pathway substrate 15	Putative tumor suppressor	-0.32429333	0.37490821	0.01111875
Fbxo11	F-box protein 11	TGF-beta signaling	-0.74050667	0.13056143	0.515905
Gli1	GLI-Kruppel family member GLI1	Primary cilium, hedgehog signaling	-5.89155	2.65261857	0.216335
Gli2	GLI-Kruppel family member GLI2	Primary cilium, hedgehog signaling	-2.301	0.16724429	0.1462125
Hey1	hes-related family bHLH transcription factor with YRPW motif 1	Neuronal differentiation	-2.52211667	0.53994524	0.298409167
Ifit2	Interferon-induced protein with tetratricopeptide repeats 2	Putative tumor suppressor	-0.59411	0.22296905	0.827468333
Kat2b	K(lysine) acetyltransferase 2B	Primary cilium, hedgehog signaling	-0.58358778	0.13037365	0.200493056
Lasp1	LIM and SH3 protein 1	Neuronal function	-1.72819852	0.71635841	0.5360575
Lrig2	leucine-rich repeats and immunoglobulin-like domains 2	Putative tumor suppressor	-0.72117667	0.61478786	0.1092475
Myo5a	myosin VA (heavy chain 12, myoxin)	Primary cilium	-0.30078444	0.03487603	0.955252222
Nedd4l	Neural precursor cell expressed developmentally downregulated gene 4-like	Putative tumor suppressor	-2.13462722	0.85995516	0.677856528
Nr3c1	nuclear receptor subfamily 3, group C, member 1 (glucocorticoid receptor)	TGF-beta signaling	-0.80474167	0.36598373	0.518120278
Otx1	orthodenticle homolog 1	Neuronal differentiation	-5.29533333	1.53385524	0.936831667
Pak1	p21 protein (Cdc42/Rac)-activated kinase 1	Neuronal differentiation	-0.77659917	0.35720762	0.474923958
Pak3	p21 protein (Cdc42/Rac)-activated kinase 3	Neuronal function	-1.569585	0.91776905	0.045022083
Pax3	paired box 3	Neuronal differentiation	-1.52859556	0.60658302	1.879074444
Pcp4	Purkinje cell protein 4, no connection to cancer	Neuronal function	-1.96301	0.43108476	1.790465833
Plxnc1	plexin C1	Neuronal function	-2.19668111	0.26895603	0.090267222
Prickle2	prickle homolog 2 (Drosophila)	Neuronal differentiation	-1.82603333	1.06802	0.3860625
Prox1	prospero homeobox 1	Putative tumor suppressor	-1.48082	0.33860921	1.261501944
Ptpn12	protein tyrosine phosphatase, non-receptor type 12	TGF-beta signaling	-0.43496333	0.09563726	0.384250833
Pvrl3	poliovirus receptor-related 3	Putative tumor suppressor	-2.19943222	0.33702564	0.322754444
Rbbp4	retinoblastoma binding protein 4	Neuronal differentiation	-0.43719333	0.25213191	0.407740208
Rbl1	retinoblastoma-like 1	Putative tumor suppressor	-0.54918833	0.39946941	0.461403958
Rnd3	Rho family GTPase 3, RhoE	Neuronal function	-1.74629667	0.24879833	0.667275833
Sema3e	sema domain, immunoglobulin domain (Ig), short basic domain, secreted, (semaphorin) 3E	Putative tumor suppressor	-1.4283275	0.33600464	0.0576525
Sema4c	sema domain, immunoglobulin domain (Ig), transmembrane domain (TM) and short cytoplasmic domain, (semaphorin) 4C	Neuronal function	-2.04957667	1.2975881	0.624894167
Sgk1	serum/glucocorticoid regulated kinase 1	Primary cilium, hedgehog signaling	-0.86358667	1.40013857	1.3462725
Smad4	SMAD family member 4	TGF-beta signaling	-0.58099444	0.04375127	0.117807222
Tgfb2	transforming growth factor, beta 2	TGF-beta signaling	-0.4909725	0.52163821	0.541501875
Zfp36l1	ZFP36 ring finger protein-like 1	Putative tumor suppressor	-2.39183667	0.77631881	0.797306667

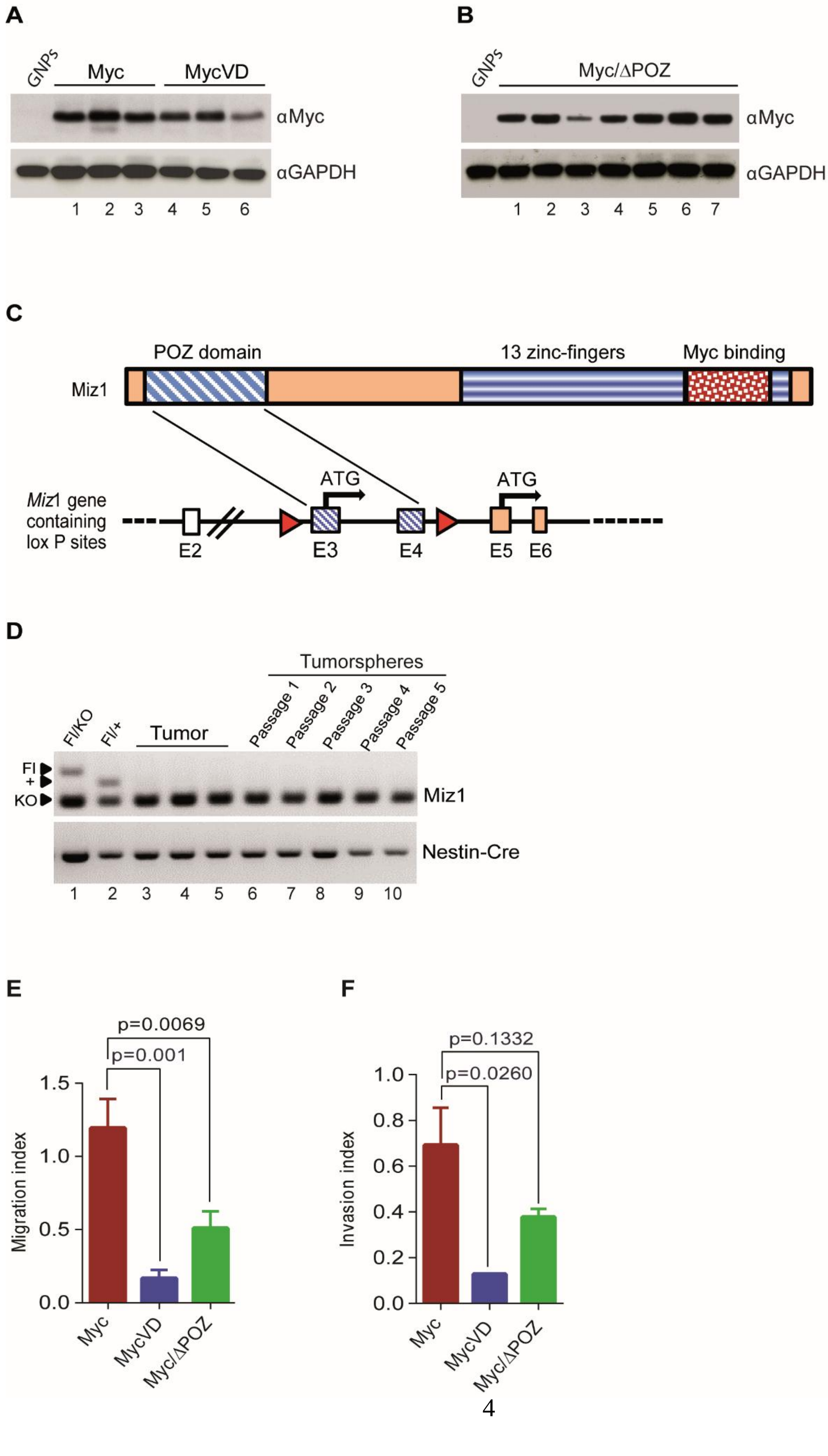
A
GNPs
Myc
MycVD
αMyc
αGAPDH
1 2 3 4 5 6
B
GNPs
Myc/ΔPOZ
αMyc
αGAPDH
1 2 3 4 5 6 7
C
POZ domain
13 zinc-fingers
Myc binding
Miz1
ATG
ATG
Miz1 gene containing lox P sites
E2
E3
E4
E5
E6
D
Tumorspheres
Fl/KO
Fl/+
Tumor
Passage 1
Passage 2
Passage 3
Passage 4
Passage 5
Fl
+
KO
Miz1
Nestin-Cre
1 2 3 4 5 6 7 8 9 10
E
p=0.0069
p=0.001
Migration index
1.5
1.0
0.5
0.0
Myc
MycVD
Myc/ΔPOZ
F
p=0.1332
p=0.0260
Invasion index
1.0
0.8
0.6
0.4
0.2
0.0
Myc
MycVD
Myc/ΔPOZ

Figure S2. Characterization of tumorspheres. Related to Figure 2. Immunoblotting of Myc expression in tumorspheres from individually derived tumors: (A) Myc (lanes 1-3) and MycVD (lanes 4-6) tumors. (B) Myc/ΔPOZ-tumors (lanes 1-7). GNPs lacking Myc expression were used as negative control. GAPDH was used as internal control. (C) Schematic of Miz1 mouse model used (Wolf et al., 2013). The POZ/BTB domain of Miz1 is encoded by exons 3 and 4 (E3, E4), which are flanked by loxP sites (red triangles). (D) Genotyping of the tail of *Miz1*$^{\Delta POZ/POZ}$*;Trp53*$^{fl/fl}$*;Nestin-Cre* mice Fl/KO versus Fl/+ (lanes 1,2), Myc/ΔPOZ tumors (lanes 3-5), tumorspheres passages 1-5 (lanes 6-10) for Miz1 deletion by the Cre recombinase. Cre was used for control. (E-F) Measurements of the migration (E) and invasion (F) properties of Myc and MycVD tumorsphere cells. p values (shown at the top) are calculated by an unpaired two-tailed t-test from 3 independent experiments. Data are represented as the mean ± SD.

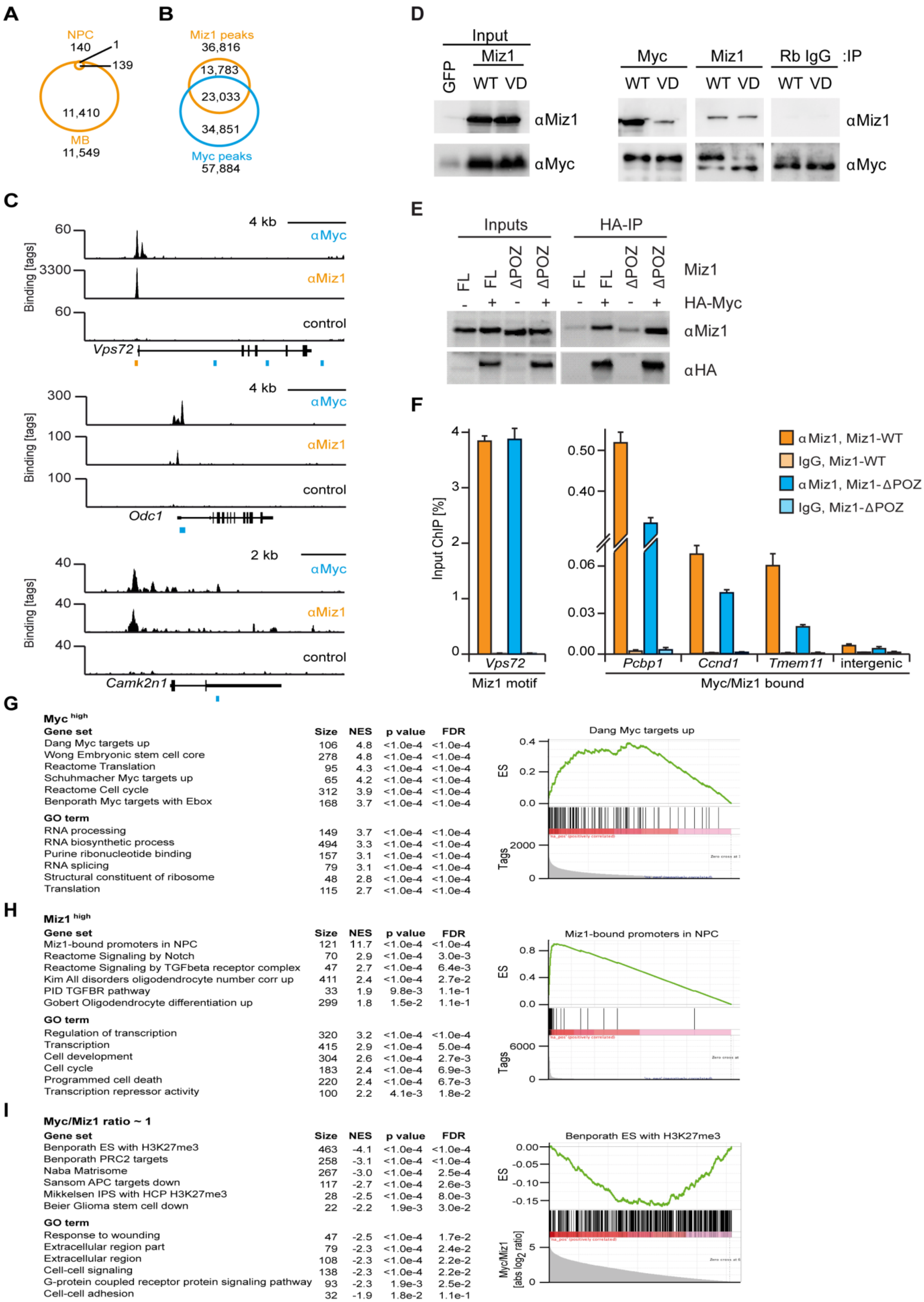
A
NPC
140
1
139
11,410
MB
11,549
B
Miz1 peaks
36,816
13,783
23,033
34,851
Myc peaks
57,884
C
4 kb
αMyc
αMiz1
control
Binding [tags]
Vps72
Odc1
2 kb
Camk2n1
D
Input
Miz1
GFP
WT VD
Myc
Miz1
Rb IgG
:IP
αMiz1
αMyc
E
Inputs
HA-IP
FL
ΔPOZ
Miz1
HA-Myc
αMiz1
αHA
F
Input ChIP [%]
αMiz1, Miz1-WT
IgG, Miz1-WT
αMiz1, Miz1-ΔPOZ
IgG, Miz1-ΔPOZ
Vps72
Miz1 motif
Pcbp1
Ccnd1
Tmem11
intergenic
Myc/Miz1 bound
G
Myc high
Gene set Size NES p value FDR
Dang Myc targets up 106 4.8 <1.0e-4 <1.0e-4
Wong Embryonic stem cell core 278 4.8 <1.0e-4 <1.0e-4
Reactome Translation 95 4.3 <1.0e-4 <1.0e-4
Schuhmacher Myc targets up 65 4.2 <1.0e-4 <1.0e-4
Reactome Cell cycle 312 3.9 <1.0e-4 <1.0e-4
Benporath Myc targets with Ebox 168 3.7 <1.0e-4 <1.0e-4
GO term
RNA processing 149 3.7 <1.0e-4 <1.0e-4
RNA biosynthetic process 494 3.3 <1.0e-4 <1.0e-4
Purine ribonucleotide binding 157 3.1 <1.0e-4 <1.0e-4
RNA splicing 79 3.1 <1.0e-4 <1.0e-4
Structural constituent of ribosome 48 2.8 <1.0e-4 <1.0e-4
Translation 115 2.7 <1.0e-4 <1.0e-4
Dang Myc targets up
ES
Tags
H
Miz1 high
Gene set Size NES p value FDR
Miz1-bound promoters in NPC 121 11.7 <1.0e-4 <1.0e-4
Reactome Signaling by Notch 70 2.9 <1.0e-4 3.0e-3
Reactome Signaling by TGFbeta receptor complex 47 2.7 <1.0e-4 6.4e-3
Kim All disorders oligodendrocyte number corr up 411 2.4 <1.0e-4 2.7e-2
PID TGFBR pathway 33 1.9 9.8e-3 1.1e-1
Gobert Oligodendrocyte differentiation up 299 1.8 1.5e-2 1.1e-1
GO term
Regulation of transcription 320 3.2 <1.0e-4 <1.0e-4
Transcription 415 2.9 <1.0e-4 5.0e-4
Cell development 304 2.6 <1.0e-4 2.7e-3
Cell cycle 183 2.4 <1.0e-4 6.9e-3
Programmed cell death 220 2.4 <1.0e-4 6.7e-3
Transcription repressor activity 100 2.2 4.1e-3 1.8e-2
Miz1-bound promoters in NPC
I
Myc/Miz1 ratio ~ 1
Gene set Size NES p value FDR
Benporath ES with H3K27me3 463 -4.1 <1.0e-4 <1.0e-4
Benporath PRC2 targets 258 -3.1 <1.0e-4 <1.0e-4
Naba Matrisome 267 -3.0 <1.0e-4 2.5e-4
Sansom APC targets down 117 -2.7 <1.0e-4 2.6e-3
Mikkelsen IPS with HCP H3K27me3 28 -2.5 <1.0e-4 8.0e-3
Beier Glioma stem cell down 22 -2.2 1.9e-3 3.0e-2
GO term
Response to wounding 47 -2.5 <1.0e-4 1.7e-2
Extracellular region part 79 -2.3 <1.0e-4 2.4e-2
Extracellular region 108 -2.3 <1.0e-4 2.2e-2
Cell-cell signaling 138 -2.3 <1.0e-4 2.2e-2
G-protein coupled receptor protein signaling pathway 93 -2.3 1.9e-3 2.5e-2
Cell-cell adhesion 32 -1.9 1.8e-2 1.1e-1
Benporath ES with H3K27me3
Myc/Miz1 [abs log2 ratio]

Figure S3. ChIP-Seq analysis of Myc and Miz1 binding sites and characterization of Myc/Miz1 interaction. Related to Figure 3. (A) Venn diagram comparing the number of Miz1 peaks in NPCs (Wolf et al., 2013) and G3 MB. (B) Venn diagram displaying the number of binding sites for Myc and Miz1 in mouse G3 MB overexpressing wild-type Myc. Only peaks which have a FDR<0.01 and contain more than 20 tags were considered as peaks. Overlapping peaks are defined as peaks in which at least one base of the Myc and Miz1 peaks are located at an identical genomic position. (C) Examples of the ChIP-Seq data for Myc and Miz1 binding to four selected genes. The traces show ChIP-Seq profiles for Miz1 and Myc in G3 MB as well as an input control for *Odc1* (a canonical Myc target gene), *Vps72* (a canonical Miz1 target gene), and *Camk2n1*. Miz1 binding motifs (orange) and canonical E-box-sequences (blue) are shown as bars below the binding traces. (D) Co-immunoprecipitation in HEK293 cells of exogenously expressed Myc with antibodies to Myc (αMyc) and Miz1 (αMiz1). Immunoprecipitation with a rabbit IgG heavy chain (Rb IgG) was used as control. (E) Co-immunoprecipitation experiment: HEK293 cells were transiently transfected with expression plasmids encoding either full-length (FL) Miz1 or Miz1ΔPOZ and HA-tagged Myc. Lysates were precipitated with αHA-antibodies. (F) ChIP experiment analyzing binding of Miz1 and Miz1ΔPOZ to target genes. Miz1 was precipitated from tumorspheres expressing either full-length or mutant (ΔPOZ) Miz1 and IgG antibody was used as a control. *Vps72* contains a consensus Miz1 binding motif. The other genes contain non-consensus E-Box and Miz1 motifs, which are bound by the Myc/Miz1 complex. Error bars indicate standard deviation. (G–I) Functional classification of direct target genes of Myc and Miz1. The number of tags in peaks within promoters was used to generate a ranked list of Myc and Miz1 target genes in mouse G3 MBs. The panels show gene sets from a GSE analysis that are highly occupied by Myc (G) or Miz1 (H). Panel I shows gene set with a ratio of Myc and Miz1 tags around 1 (see plot in

Figure 3). Gene sets and GO terms were taken from the MSig data base (C2 and C5) and spiked with a gene set of Miz1-bound promoters in mouse neuronal progenitor cells (Wolf et al., 2013). For each table one enrichment plot is shown (right).

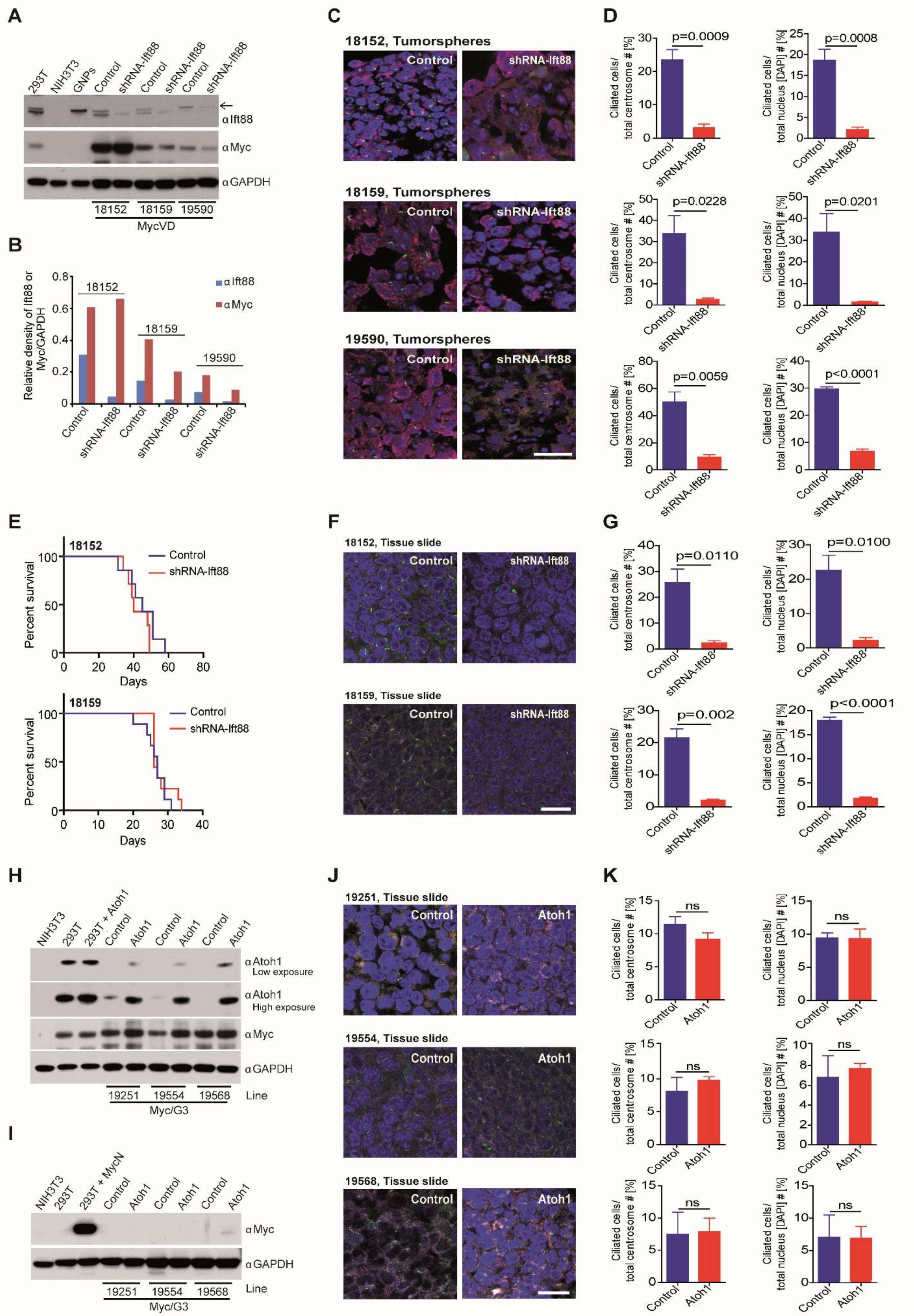
A
293T
NIH3T3
GNPs
Control
shRNA-Ift88
αIft88
αMyc
αGAPDH
18152
18159
19590
MycVD
B
Relative density of Ift88 or Myc/GAPDH
αIft88
αMyc
C
18152, Tumorspheres
18159, Tumorspheres
19590, Tumorspheres
D
Ciliated cells/ total centrosome # [%]
Ciliated cells/ total nucleus [DAPI] # [%]
p=0.0009
p=0.0008
p=0.0228
p=0.0201
p=0.0059
p<0.0001
E
Percent survival
Days
F
18152, Tissue slide
18159, Tissue slide
G
p=0.0110
p=0.0100
p=0.002
p<0.0001
H
293T + Atoh1
Atoh1
αAtoh1 Low exposure
αAtoh1 High exposure
19251
19554
19568
Line
Myc/G3
I
293T + MycN
J
19251, Tissue slide
19554, Tissue slide
19568, Tissue slide
K
ns

L

Geneset	NES	p value	q value
Reactome: Pre *NOTCH* transcription and translation	-2.35	$<1.0 \times 10^{-4}$	$<1.0 \times 10^{-4}$
KEGG: *NOTCH* signaling pathway	-2.14	$<1.0 \times 10^{-4}$	5.0×10^{-4}
Reactome: *BMAL1/CLOCK/NPAS2* activates circadian expression	-1.89	1.2×10^{-3}	1.1×10^{-2}
PID: Hedgehog *GLI* pathway	-1.88	$<1.0 \times 10^{-4}$	1.1×10^{-2}
Reactome: Circadian clock	-1.86	1.2×10^{-3}	1.4×10^{-2}
Biocarta: SHH pathway	-1.82	2.8×10^{-3}	1.9×10^{-2}

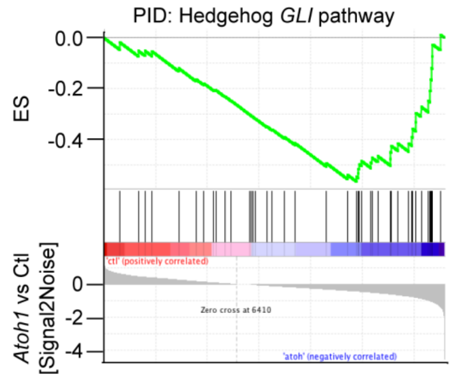

M

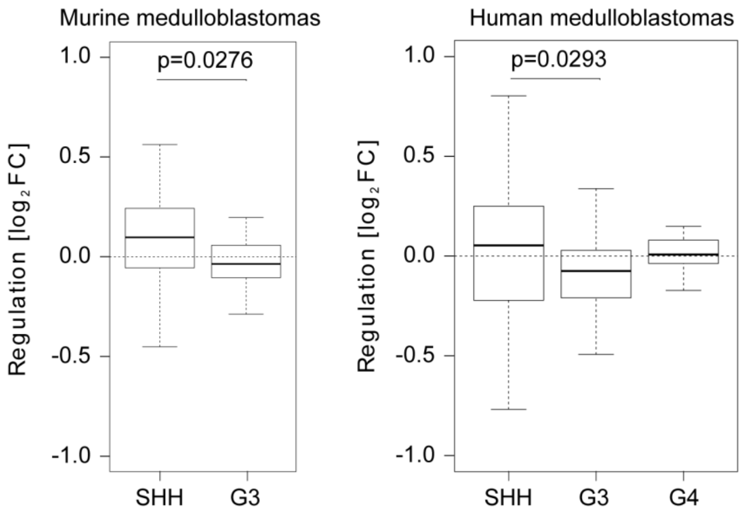

Figure S4. Knock down primary cilia in MycVD mutant tumorpheres in vitro and in vivo. Related to Figure 4. (A) Immunoblotting of Ift88 and Myc protein expression from three individual MycVD mutant tumorsphere lines (18152, 18159, and 19590). GAPDH was used as internal control. (B) Densitometry measures the relative density of Ift88 and Myc over GAPDH in panel S4A. (C) Detection of primary cilia from three individual MycVD mutant tumorspheres by immunofluorescence with an antibody to Arl13b (green) detecting primary cilia and to γ-tubulin (purple) to identify basal bodies. DAPI (blue) was used to detect nuclei. Scale bar = 50 μm. (D) Percentages of ciliated cells: the number of the basal body or nuclei was used as a denominator to calculate the percentage of ciliated cells. p values compared MycVD tumorspheres (control) to MycVD tumorspheres overexpressing the shRNA of Ift88 (shRNA-Ift88). (E) Kaplan-Meier survival curves of mice transplanted with two of the three individual MycVD mutant tumorsphere lines (18152 and 18259) infected with control (blue) and shRNA-Ift88 (red) encoding retroviruses. Median survival (ms) for line #18152; control was 43 days (n = 6) and shRNA-Ift88 40 days (n = 7). Median survival (ms) for line #18159; control was 27 days (n = 9) and shRNA-Ift88 26 days (n = 9). (F and G) Detection and percentages of primary cilia from tumor sections as described previously. p values (shown at the top) were calculated by an unpaired two-tailed t-test. Scale bar = 50 μm. (H and I) Immunoblotting of Atoh1, Myc, and MycN expression in three individual G3 tumorsphere lines (19251, 19554, and 19568) infected with Atoh1 encoding retroviruses. NIH3T3 cells were used as negative control. 293T cells were transfected with Atoh1 or MycN and used as positive controls. GAPDH was used as internal controls. (J and K) Immunofluorescence of primary cilia from tumor sections as described in (C and D). Scale bar = 50 μm. No significant "ns" difference between control vs. Atoh1 overexpression. (L) Selected gene sets of a GSE analysis of Atoh1 overexpressing G3 MBs compared to control G3 MBs. These gene sets are enriched for activated genes after Atoh1 overexpression. One representative enrichment plot is shown on the right. (M) Box plot illustrating discrimination of murine (left) and human (right) SHH and G3 MBs by a gene set of SHH pathway members. The gene set "PID: Hedgehog *GLI* pathway" was taken from the C2 collection of the MSigDB. Gene expression data from murine (GSE33199) and human (GSE37382) MB subgroups were median centered and expression of each gene in the gene set was averaged within each subgroup. The black line indicates the median value, bottom and top of the boxes reflect first and third quartile, whiskers represent 1.5 interquartile range, and outliers are not shown (Tukey box plot). p values were calculated using a paired two-tailed Wilcoxon signed-rank test. Data in graphs D, G, and K represent the mean ± SD.

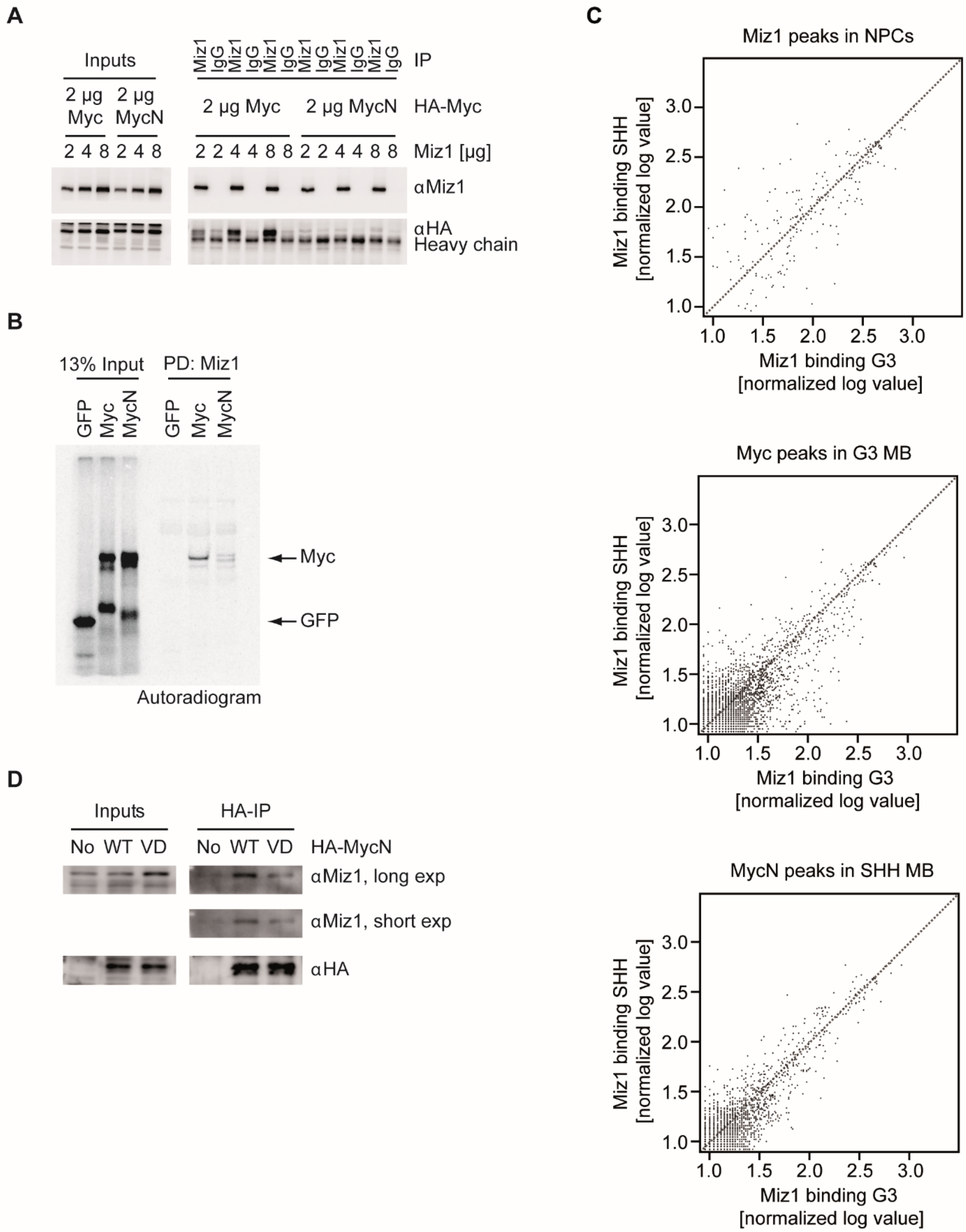
A
Inputs
IP
Miz1 IgG Miz1 IgG Miz1 IgG Miz1 IgG Miz1 IgG Miz1 IgG
2 µg Myc
2 µg MycN
2 µg Myc
2 µg MycN
HA-Myc
2 4 8 2 4 8
2 2 4 4 8 8 2 2 4 4 8 8
Miz1 [µg]
αMiz1
αHA
Heavy chain
B
13% Input
PD: Miz1
GFP Myc MycN GFP Myc MycN
Myc
GFP
Autoradiogram
C
Miz1 peaks in NPCs
Myc peaks in G3 MB
MycN peaks in SHH MB
Miz1 binding SHH [normalized log value]
Miz1 binding G3 [normalized log value]
1.0 1.5 2.0 2.5 3.0
D
Inputs
HA-IP
No WT VD
No WT VD
HA-MycN
αMiz1, long exp
αMiz1, short exp
αHA

Figure S5. Miz1 binding to Myc target genes is stronger in tumorspheres from G3 MB than in SHH MB. Related to Figure 5. (A) Co-immunoprecipitation experiments from HEK293 cells expressing HA-tagged versions of Myc (MycN or Myc) together with increasing amounts of Miz1. Mouse IgG was used as control. (B) Interaction assay with recombinant Miz1 protein. GFP, MycN and Myc were translated in vitro in the presence of $^{[35]}$S-methionine or -cysteine and precipitated with recombinant GST-tagged Miz1 that had been purified from *E. coli*. Precipitated proteins were detected by autoradiography. (C) Comparison of normalized binding strengths of Miz1 binding in SHH MB tumorspheres (Y axis) to Miz1 binding in G3 tumor cells (X axis) versus Miz1in NPCs (top panel), Myc in G3 tumor cells (middle panel) and MycN in SHH MB tumorspheres (bottom panel). Each dot represents Miz1 binding strength to one gene. (D) Co-immunoprecipitation between HA-tagged MycN (WT) and HA-MycNVD (VD) with Miz1 both co-expressed in HEK293 cells immunoblotted with antibodies to Miz (long and short exposure) and to HA.

Human G3 medulloblastomas

Oncogenic signature	Size	NES	p value	FDR
E2F1_up.V1_up	182	4.4	<1.0e-5	<1.0e-5
PDGF_up.V1_up	140	4.1	<1.0e-5	<1.0e-5
VEGF_A_up.V1_up	188	3.5	<1.0e-5	<1.0e-5
RB_p130_dn.V1_dn	134	3.4	<1.0e-5	<1.0e-5

Murine G3 medulloblastomas (MycWT-activated)

Oncogenic signature	Size	NES	p value	FDR
KRAS.amp.lung_up.V1_up	100	-1.5	1.7e-3	3.9e-2
LEF1_up.V1_up	167	-1.5	1.6e-3	3.9e-2
EGFR_up.V1_up	171	-1.5	3.2e-3	4.6e-2
WNT_up.V1_up	158	-1.5	4.8e-3	5.7e-2

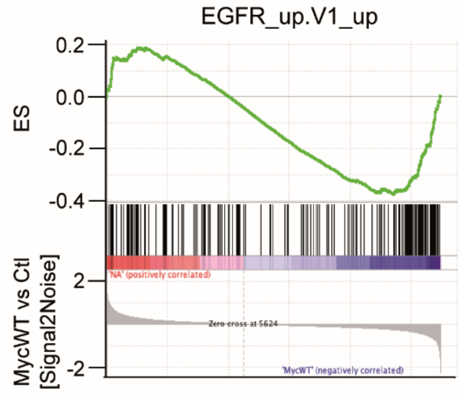

Figure S6. GSEA of human and murine G3 MBs. Related to Figure 6. Oncogenic signatures were taken from the C6 MsigDB. Gene expression of human MBs (Northcott et al., 2012) was median centered and ranked. For murine MBs gene expression changes of Myc-transduced versus control tumors have been compared. One enrichment plot is displayed on the right.

Supplemental Experimental Procedures

Antibodies used for immunofluorescence and immunoblotting.

Name	Supplier	Catalog no.	Dilution	Application
Ki67	Leica	NCL-Ki67P	1:1000	IF
Caspase-3	Biocare Medical	CP229A	1:250	IF
Arl13b	NeuroMab	N295B/66	1:2000	IF
γ-tubulin	Sigma	T5192	1:1000	IF
Ift88	Proteintech	13967-1-AP	1:1000	IB
Atoh1	Abcam	Ab105497	1:1000	IF
Atoh1	Abcam	Ab 168374	1:1000	IB
Myc	Abcam	Ab32072	1:500	IF
Myc	Cell Signaling	9402S	1:1000	IB
MycN	Santa Cruz Biotechnology, Inc.	SC-53993	1:200	IB
GAPDH	Applied Biosystems, Ambion	AM4300	1:5000	IB
β-actin	Santa Cruz Biotechnology, Inc.	SC-1615	1:2000	IB
Myc	Santa Cruz Biotechnology, Inc.	SC-764	1:1000	IB
HA	Santa Cruz Biotechnology, Inc.	SC-805	1:1000	IB, IP
Miz1	Martin Eilers Group	10E2	1:500	IB, IP

IF = Immunofluorescence, IB = Immunoblotting, IP = Immunoprecipitation

Mouse Genotyping

Genotyping of mice was performed using the following primers:

Miz-1 intron 2: 5'– GTATTCTGCTGTGGGGCTATC –3'

Miz-1 exon 3: 5'– GGCTGTGCTGGGGGAAATC –3'

Miz-1 intron 4: 5'– GGCAGTTACAGGCTCAGGTG –3'

Nestin: 5'– GATGAAGCAGGAACCCCGGTTGCGTG –3'

Cre reverse: 5'– TCGTTGCATCGACCGGTAATGCAGGC –3'

Primers for ChIP assays. Related to Figure 5 and Figure S3.

1. *Pcbp1* Forward: CGCGCACGTTTTCGAC
   Reverse: GATGGCGGAGCGATACAG

2. *Ccnd1* Forward: GCGTCCTCAGGCTCTCG
   Reverse: CCACGTGGTCGTCCTGA

3. *Tmem11* Forward: TGTGTCTGGGTGTTTTGTGC
   Reverse: GTAACGTCTGACGCCCTCTT

4. Intergenic Forward: GAATGTGGCCAGTGGACTTT
   Reverse: ATCCTAAGCTTCCCCTCCAG

Orthotopic transplants

Transplantation of Myc-, MycN-, MycVD- or MycNVD-infected GNPs or tumor cells into the cerebellum or cortices of recipient mice yielded similar times of onset, incidence, and phenotypic characteristics of MB development. Our rationale for the number of cells injected into the cortices of recipient mice to examine the oncogenic potential of *Myc* was based on our previous experiments (Ayrault et al., 2010).

Cell Migration and Invasion Assays

The outside of the transwell insert membrane was coated with 50 µl rat tail collagen (50 µg/ml) overnight at 4°C. The next day, aliquots of rat tail collagen (50 µl) were added into the transwell inserts to coat the inside of the membranes for 1.5 hr at room temperature. Cells were harvested from cell culture dishes by accutase into 15 ml conical tubes and centrifuged at 800 x g for 5 min. Cell pellets were resuspended in complete neurobasal medium supplemented with 0.2% BSA at a cell density of 3×10^4 cells/ml. Aliquots of 100 µl cell suspension were loaded into transwell inserts that were subsequently placed into the 24-well plate. The transwell insert-loaded plate was placed in a cell culture incubator for 5 hr. For invasion assay, inserts (BD Biosciences) were coated with 50 µl of a 1:4 Matrigel/Medium dilution (BD Biosciences) and allowed to solidify at 37°C for 1 hr. Cells were resuspended (3 x 10^4 cells/ml) in complete neurobasal medium supplemented with 0.2% BSA and 500 µl of cell suspension were added to each insert and allowed to invade through a porous membrane coated with Matrigel at 37°C for 24 hr. For migration and invasion assays, the cells inside transwell inserts were removed by cotton swabs. The cleaned inserts were fixed in 300 µl of 4% paraformaldehyde (pH 7.5) for 20 minutes at room temperature. Cells which had migrated to the outside of the transwell insert membrane were stained using HEMA 3 staining kit (Fisher Scientific Inc, TX). The number of stained cells was counted as previously described (Vo and Khan, 2011; Zigmond et al., 2001). Results were expressed as migration/invasion index defined as the average number of cells per field. The experiments were conducted at least three times using independent cell preparations.

Affymetrix Microarray Analysis

Comparison with other mouse MBs subgroups, used Affymetrix Mouse Genechips HT430 V2 as previously described (Ayrault et al., 2010; Kawauchi et al., 2012). For each probe set, subject Z-scores were calculated by computing the mean and standard deviation across subjects within each probe set.

Functional analysis of gene sets was performed using DAVID (Huang da et al., 2009). Gene set enrichment analysis (GSEA) (Subramanian et al., 2005) was performed (1,000 permutations) with the C2 and C6 gene sets from the MSigDB (http://www.broadinstitute.org/gsea/msigdb). Heatmaps were generated using RMA-normalized data downloaded from GEO (GSE33199). Probes matching the same gene were de-duplicated by the median. Log_2FC were calculated by substracting the median of the whole dataset from log_2

intensity values and subsequently normalized to +/-1. Heatmaps were plotted using MeV v4.8.1 (Saeed et al., 2003). For expression profiles of human MBs raw data were downloaded from GEO (GSE37382), RMA-normalized using the affy package in R and probes without matching gene symbols were removed. Log_2FC were calculated by substracting the median of the whole dataset from log_2 intensity values.

RNA-Sequencing Analysis

Reads were sequentially mapped using an in-house script implementing BWA with default settings, STAR (extra settings: "--outSAMunmapped Within --outSAMstrandField intronMotif") and SIM4 with default settings, followed by a re-implementation of Picard's CleanSam in which alignments that run off the end of the reference were trimmed and extended by identifying soft-clipping that could align in-place.

Reads for each ensembl gene were counted using the summarizeOverlaps {Genomic Alignments} function in R (R Core Team, 2015). Weakly expressed genes were removed (read sum of all samples per gene > 14) and differentially expressed genes were called using edgeR (Robinson et al., 2010).

ChIP-Sequencing Analysis

Downstream analyses were performed using R and Microsoft Excel (or programs described later). Binding profiles were visualized using the Integrated Genome Browser software (Nicol et al., 2009). To create density distributions (heatmaps) indicating co-occupancies of binding sites, Seqminer v.1.3.3 (Ye et al., 2011) was used (to avoid 0 tags, 1 was added to all values). Peak annotations were achieved using the 'closestBed' feature from the Bedtools suite v.2.11.2 (Quinlan and Hall, 2010) and the UCSC GoldenPath RefSeq database for murine (mm9) genes. Intersections of ChIP-sequencing peaks were done with the 'intersectBed' tool from Bedtools and default parameters. GSEA preranked analyses were performed to identify specific gene sets enriched in strongly Myc- and Miz1-bound genes in murine G3 MBs. Therefore, genes with a ChIP-Seq peak within +/-5kb around a transcriptional start site (TSS) were selected and the numer of tags in the peak was used to generate a ranked gene list that was subsequently used for gene set enrichment analyses (default settings) with the C2 and C5 collection of the MSigDB. For Myc/Miz1 joint peaks the absolute $\log_2$ Myc/Miz1 ratio was calculated, a ranked gene list was built and subjected to GSEA preranked analysis with default parameters.

In vitro transcription and translation assays (IVT)

For the in vitro interaction assays, GFP, MycN and Myc were expressed with the T7 Quick Coupled Transcription/Translation System (Promega). 30 µl of reticulocyte-lysate was mixed with 1 µg of CMV-plasmid-DNA and 2 µl of [35S]-methionine (1,000Ci/mmol at 10mCi/ml) and incubated for 90 min at 30°C. GST-tagged Miz1 was expressed from a pGEX4T-plasmid in Bl-21 in 50 ml LB-culture and expression was induced with a final concentration of 0.5 mM IPTG for 3 h at 30°C. Bacterial Cells were resuspended in 2 ml PBS containing protease inhibitors and a final concentration of 0.1 % of NP-40. Cells were disrupted by sonication and the soluble fraction was incubated with 200 µl of Glutathione Sepharose (GE) for 3 h at 4°C to immobilize GST-Miz1. 20 µl of GST-Miz1-beads were incubated with 15 µl of [35S]-methionine-labelled proteins for 150 min at 4°C. Labelled proteins in eluates and inputs were separated by SDS-PAGE gels and visualized by autoradiography.

Statistical Analysis

The Kaplan-Meier method was used calculate the significance of mouse survival. Statistical analyses were performed in the GraphPad Prism software version 6.0 or R.

Supplemental References

Huang da, W., Sherman, B. T., and Lempicki, R. A. (2009). Systematic and integrative analysis of large gene lists using DAVID bioinformatics resources. Nat. Protoc. *4*, 44-57.

Nicol, J. W., Helt, G. A., Blanchard, S. G., Jr., Raja, A., and Loraine, A. E. (2009). The Integrated Genome Browser: free software for distribution and exploration of genome-scale datasets. Bioinformatics *25*, 2730-2731.

Quinlan, A. R., and Hall, I. M. (2010). BEDTools: a flexible suite of utilities for comparing genomic features. Bioinformatics *26*, 841-842.

R Core Team (2015). R: A language and environment for statistical computing. R Foundation for Statistical Computing, Vienna, Austria. URL http://www.R-project.org/

Robinson, M. D., McCarthy, D. J., and Smyth, G. K. (2010). edgeR: a Bioconductor package for differential expression analysis of digital gene expression data. Bioinformatics *26*, 139-140.

Saeed, A. I., Sharov, V., White, J., Li, J., Liang, W., Bhagabati, N., Braisted, J., Klapa, M., Currier, T., Thiagarajan, M., *et al.* (2003). TM4: a free, open-source system for microarray data management and analysis. Biotechniques *34*, 374-378.

Subramanian, A., Tamayo, P., Mootha, V. K., Mukherjee, S., Ebert, B. L., Gillette, M. A., Paulovich, A., Pomeroy, S. L., Golub, T. R., Lander, E. S., and Mesirov, J. P. (2005). Gene set enrichment analysis: a knowledge-based approach for interpreting genome-wide expression profiles. Proc. Natl. Acad. Sci. U. S. A. *102*, 15545-15550.

Vo, B. T., and Khan, S. A. (2011). Expression of nodal and nodal receptors in prostate stem cells and prostate cancer cells: autocrine effects on cell proliferation and migration. The Prostate *71*, 1084-1096.

Ye, T., Krebs, A. R., Choukrallah, M. A., Keime, C., Plewniak, F., Davidson, I., and Tora, L. (2011). seqMINER: an integrated ChIP-seq data interpretation platform. Nucleic Acids Res. *39*, e35.

Zigmond, S. H., Foxman, E. F., and Segall, J. E. (2001). Chemotaxis assays for eukaryotic cells. Current protocols in cell biology / editorial board, Juan S Bonifacino et al. *Chapter 12*, Unit 12-11